Demonstration of time-of-flight technique with all-optical modulation and MCT detection in SWIR/MWIR range

Kaplan, Andre; Wu, Rihan; Collins, Jack; Burgess, C; Lamb, R

DOI:
10.1117/12.2500326

Document Version
Peer reviewed version

Demonstration of time-of-flight technique with all-optical modulation and MCT detection in SWIR/MWIR range

Kaplan, Andre; Wu, Rihan; Collins, Jack; Burgess, C; Lamb, R

DOI:
10.1117/12.2500326

Document Version
Early version, also known as pre-print

Citation for published version (Harvard):
Kaplan, A, Wu, R, Collins, J, Burgess, C & Lamb, R 2018, 'Demonstration of time-of-flight technique with all-optical modulation and MCT detection in SWIR/MWIR range' Proceeding of SPIE, vol. 10799, 1079904. DOI: 10.1117/12.2500326

Demonstration of time-of-flight technique with all-optical modulation and MCT detection in SWIR/MWIR range

Conference Paper · October 2018

DOI: 10.1117/12.2500326

CITATIONS
0

READS
68

5 authors, including:

Jack Collins
University of Birmingham
3 PUBLICATIONS **0** CITATIONS
SEE PROFILE

Andrey Kaplan
University of Birmingham
34 PUBLICATIONS **287** CITATIONS
SEE PROFILE

Rihan Wu
University of Birmingham
4 PUBLICATIONS **3** CITATIONS
SEE PROFILE

Demonstration of Time-of-Flight technique with all-optical modulation and MCT detection in SWIR/MWIR range

Rihan Wu[a], Jack Collins[a], Christopher D. Burgess[b], Robert A. Lamb[c] and Andrey Kaplan[a]

[a]School of Physics and Astronomy, University of Birmingham, Birmingham, B15 2TT, UK;
[b]Dstl, Porton Down, Salisbury, SP4 0JQ, UK;
[c]Leonardo MW Ltd, 2 Crewe Road North, Edinburgh, EH5 2XS, UK

ABSTRACT

We report a feasibility study of Time-of-Flight technique in Short- and Mid-Wavelegth Infrared spectral region using a Mercury Cadmium Telluride detector. For the demonstration we employed an all-optical modulator operated by optical pumping with 800 nm, 100 femtosecond pulses and measured the broadening of the signal pulses traversing through a few centimetres of silica rod. The measured signal was analysed to reconstruct the pulse broadening and to retrieve the group velocity dispersion of silica. We show that in Time-of-Flight measurements based on all-optical modulation in combination with Mercury Cadmium Telluride detector, the limiting resolution factor is the speed of the modulator rise time governed by the optical pump.

Keywords: Time-of-Flight, far-IR, modulation, switching, group velocity dispersion

1. INTRODUCTION

Range-finding and 3D imaging provides information about the distance to an object in addition to the standard intensity received by detector or camera. Since the first Time-of-Flight (ToF) imager was demonstrated,[1] it became apparent that this active measuring technique offers advantages over passive and active triangulation.[2,3] The ToF technique resolves ambiguity problems related to projected fringes, contrastless scenes and high computational cost. To employ ToF range-finding, it is possible to modulate either pulse, amplitude or frequency. In the pulse modulation method the time of arrival of the pulse reflected from the target is measured[4] and it has been shown theoretically to provide the best precision.[5]

In recent decades, the main development of ToF imaging and distance measurement was reported for the visible and near-IR ranges and the technology rapidly matured to provide commercially available products. However, similar achievements in far-IR have not yet materialised despite clear technological advantages the ToF technique can offer in this range. One of the problems is the ultrafast gating of the detectors operating in the far-IR, which at their best can achieve a few nanoseconds, more than an order of magnitude slower than their counterparts in the visible range.[6] Nevertheless, several successful applications have been reported, such as integrated path differential absorption lidar operating for active sensing of CO_2 developed by DRS Technologies in collaboration with NASA[7] or the airborne CO_2 Sounder lidar.[8]

On the other hand, a reliable detection method is important for the ToF applications and the major players in far-IR imaging industry, such as Leonardo, Raytheon, Sofradir and SCD consider Mercury Cadmium Telluride (MCT) as a semiconducting material with noticeable advantages over other rivals, such as InSb. MCT detectors offer a better range of detection, resolution, device size and performance-to-cost value. MCT is the only known detector material which covers the spectral ranges of short, mid and long wavelength IR (SWIR, MWIR and LWIR). Because of its robust performance, MCT became an integral part in the most demanding applications in the battlefield, as in the Phalanx CIWS shipboard defence system operating in LWIR and DIRCM countermeasure sensors for protecting military aircrafts in MWIR. Therefore, a natural development would be the integration of MCT detectors into an active measurement and imaging device using the ToF technique. MCT has demonstrated the ability to produce clear signal in the scene flooded with photons and where the parasitic

Further author information: (Send correspondence to A.K.)
A.K.: E-mail: a.kaplan.1@bham.ac.uk

reflection can be discriminated from useful ones by gating and filtering photons arriving before or after those reflected from the useful target.

Our work aims to demonstrate the feasibility of ultrafast ToF measurements using an MCT detector with an all-optical modulator operating in the SWIR/MWIR range. The principle of the modulator work was reported previously.[9–11] Briefly, the core of the modulator is a silicon photonic membrane consisting of 2D periodically arranged holes. Due to the photonic properties of the structure, the membrane reflects less and transmits more IR light than a bare silicon window of the same thickness. However, when an external optical source optically excites the membrane by pumping free electrons, it resonates at a predesigned wavelength in such way that its reflectance increases and transmittance drops. The change is related to the alteration of the effective dielectric function by the excited free electrons. Using an external pulsed pump source, it is possible to modulate a synchronous response of the membrane, switching it between the fully transmitted and opaque states. The modulated membrane is positioned in front of the detector and acts as a shutter which can be activated synchronously with a pulse from an external optical source. Such arrangements allow us to use detectors with a slow response as the resolution is determined by the response of the modulator. We have shown previously that it is possible to achieve almost 100% modulation contrast in MWIR ranges pumping the free carrier density of $10^{18} - 10^{19}$ cm^{-3}. The speed of the modulation is limited by the pulse properties of the pump source and the free carrier lifetime. In this work we used a 100 femtosecond laser as pump source, which defines the rise time of the modulator. The life time of the free carriers is in the range of a few tens of nanoseconds or shorter due to Auger recombination which determines the time required for the modulator to return to its initial transparent state. The recovery time in such a set-up determines the repetition rate at which the modulator can be potentially used.

In this paper we show that a modulator driven by a 100 femtosecond pump pulse provides speed corresponding to the ToF resolution of a few tens of micrometers and allows the measurement of the subtle effects of a pulse broadening by Group Velocity Dispersion (GVD) in a few centimetre long silica rod. For the demonstration, a set-up was constructed providing an 800 nm pump pulse used to modulate the transmittance of the optical membrane. Another pulse, tunable in the range between 2.1 and 3.5 μm and synchronised with the pump, was used to evaluate the ToF through free space and the retardation induced by the insertion of a few centimetres long silica rod into the optical path. Both the pulse broadening (caused by propagation through the rod) and the GVD of silica were estimated from the signal received by the detector.

2. EXPERIMENT

In brief, the laser system delivers a 800 nm, 3 W pulse with a repetition rate of 1 kHz and a FWHM of about 100 fs with nearly Gaussian shape as measured using an intensity autocorrelator. A beam splitter was used to split the beam into reflected and transmitted components with the intensity ratio of 1:10. The reflected beam was further attenuated using a combination of a half-wave plate and a linear polarizer. After the attenuator, this component was used as a pump pulse to tune the optical properties of the membranes changing their reflectance and transmittance. The beam transmitted by the beam splitter was guided into an optical parametric amplifier (OPA) to generate a tunable "signal" pulse in the SWIR/MWIR, covering the range between 2.1 and 3.5 μm. The spectral range in these experiments is limited by the transmission window of the silica rods used for stretching the signal pulse. In particular, at wavelengths shorter than 2.1 μm the signal is absorbed by –OH vibrating groups found in silica, while the cut–off wavelength longer than 3.5 μm is related to IR-active absorption of Si–O bond.[12] In-between those wavelengths the rods are semitransparent for the signal. More detailed information about the system can be found elsewhere.[10,13,14] To construct the ToF, the arrival times of the 800-nm-pump and SWIR/MWIR signal pulses have to be synchronised. The synchronisation by the optical setup is shown in Fig. 1.

The diagram shows optical paths of the pump and signal pulses. The red line designates the pump whose arrival time at the optical membrane (3) can be changed by a retroreflector mounted on a computer-controlled translational stage (2). The green line marks the signal pulse delivered by the OPA. The signal passes through a silica rod (1), which delays and stretches the pulse, before it traverses the membrane. After the membrane any unabsorbed pump light that is transmitted through the membrane is rejected by a longpass filter (4), allowing only the signal to pass through. The signal is detected by a Teledyne Judson J15 photoconductive Mercury Cadmium Telluride detector (5) connected to a Zurich Instrument lock-in amplifier.

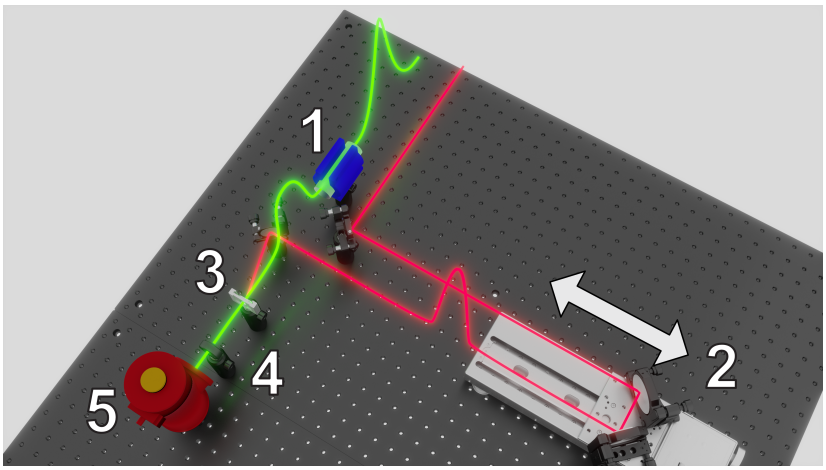

Figure 1. ToF feasibility demonstrator. Green and red lines show schematically the optical paths of the signal and pump pulses, respectively. (1) 5 or 10 cm silica rod aimed to stretch the signal pulse delivered by the OPA; (2) retroreflector mounted on a translational stage synchronising the arrival of the pump and signal pulses at the surface of the tunable optical membrane (3); (4) longpass filter blocking the pump; (5) MCT detector.

The optical membranes used in this work are similar to those presented in our report.[11] Briefly, the optical membranes were made by photoelectrochemical etching of ordered 2D hole array in a thin (a few tens of microns) silicon slab using HF acid. A fabrication procedure employed in this work is similar to that described previously.[15] In this work we used a membrane which was ∼63 μm thick, containing an ordered pattern of 1 μm holes separated by 1.5 μm and arranged into a hexagonal 2D lattice. The membrane geometry and layout were computer simulated and tested in the lab to optimise the modulation performance in the SWIR/MWIR range.

3. RESULTS AND DISCUSSION

To set-up the ToF measurements we initially removed the silica rod from the signal's optical path and adjusted the position of the retroreflector in such a way that the pump and signal pulses arrive simultaneously on the surface of the membrane, that is when the membrane is activated and the transmission of the signal is suppressed. This position can be regarded as the relative zero-distance and it is nearly identical for all wavelengths of the signal, as the dispersion of air is insignificant to change the speed of light and the arrival time of the pulse at the surface of the membrane. After the silica rod was inserted into the path the ToF of the signal is delayed, because the propagation speed slows down inside the rod. The position of the retroreflector was readjusted accordingly to add an additional distance D to the optical path of the pump for compensating the added ToF in the optical path of the signal. At this new position the pump and signal again arrive simultaneously on the surface of the membrane, blocking the passage of the latter. This procedure was repeated for different wavelengths and lengths of the rod. In such way, by scanning the retroreflector position, a ToF delay with respect to the zero position, induced by the rod, can be found as:

$$ToF = (n(\lambda) - 1)\frac{L}{c} = \frac{D}{c}, \tag{1}$$

where $n(\lambda)$ is the wavelength-dependent refractive index of the rod, L is the length of silica rod and c is the speed of light in vacuum.

Fig. 2 summarises the results showing the signal intensity as a function of the distance D added to pump optical path (bottom x-axis) and the corresponding ToF (top x-axis). The blue dots show the signal travelling along the optical path without passing through the rod. The green and red dots demonstrate the delay of the ToF because of the insertion of 5 and 10 cm long rod, respectively. (We note, silica has very poor transmission beyond the wavelength of 3 μm, thus it was not possible to use the 10 cm silica rod.) It can be seen that the insertion of the 5 cm long rod delays the ToF by about 75 picoseconds (we remark that this time depends on the

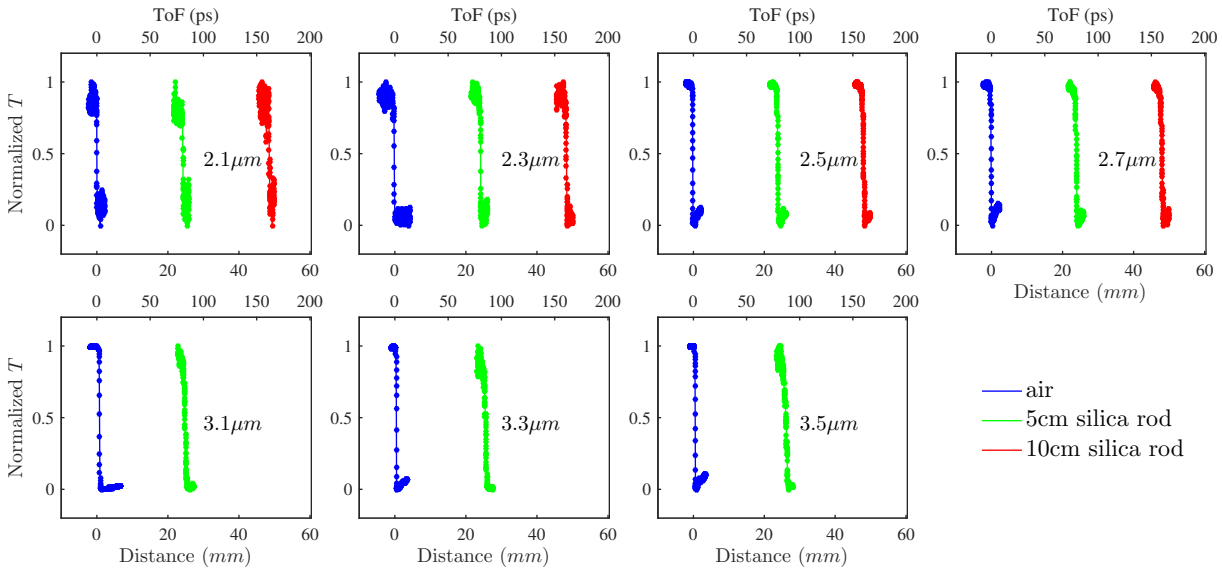

Figure 2. Normalised intensity of the transmitted signal at different wavelengths in the range between 2.1 and 3.5 μm. Blue colour represents the result of the signal passing through free space without a silica rod; green - with a 5 cm rod; red - with a 10 cm rod.

wavelength because of the silica rod dispersion). This time gets longer when the rod length is twofold increased to 10 cm, as shown by the red dots.

However, the ToF demonstration is not limited to the measurements of the arrival times, it can be further expanded to show that the setup can be used to measure the GVD of the silica rod from the analysis of the signal waveform. Fig. 3 shows the normalised intensity of the transmitted signal at selected wavelengths in the range between 2.1 and 3.5 μm as a function of time between the signal and pump. In fact the data can be viewed as similar to that shown in Fig. 2, but presented at higher resolution and shifted on the time-scale to overlap the dropping edges for easier comparison. The point of such presentation is to show the signal pulse stretching after propagation through the rod in comparison to that passing through free space. The measurements of the signal pulse stretching at each wavelength was preceded by evaluation of the membrane temporal response (shown as blue dots). This was done by recording the signal transmitted by the membrane as a function of the delay time between the pump and signal pulses without the silica rod in the optical path. The temporal response curve comprises of three regions corresponding to: negative time when the signal arrives before the pump pulse and when the membrane is nearly fully transparent; around zero-delay when the arrival time of both pulses is almost coincident and when the transmittance of the membrane is rapidly suppressed by the pump excitation; positive time when the signal arrives after the pump and when the membrane is not transmitting the signal. The temporal resolution of the ToF is determined by the second region, that is the time during which the transparency of the membrane switched between the two states of transmitting or rejecting the incoming signal. It can be seen from Fig. 3 that the response time is below 100 femtosecond and nearly independent of the wavelength. Because the response time is set by the speed of the excitation, we conclude that the excitation by the pump is an instant process and that the rising edge of the pump pulse governs the speed of the membrane modulation. At the positive times, the membrane's transmittance tends to return to its original state. However, the observation and measurements of the full recovery is not shown in this work as it happens on much longer time scales of a few hundred picosecond, as was reported previously by us.[11]

Fig. 3 shows that the signal response is stretched from an "instantaneous" to a few picosecond long response when a silica rod of 5 or 10 cm long, green and red lines, respectively, is inserted into the optical path (see Fig. 1). The observed broadening of the signal response curve is a result of the dependence of the group velocity on the frequencies comprising traversing through the rod pulse, that is GVD is responsible for stretching the signal emerging from the rod. The duration of the stretched pulse, τ, is related to the original pulse as the following:[16]

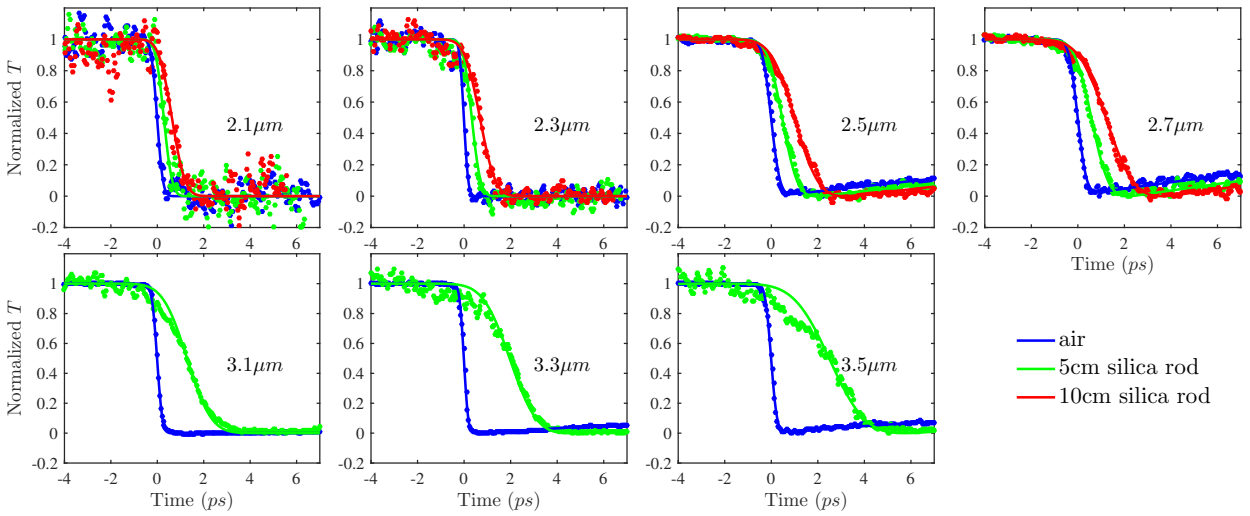

Figure 3. Normalised intensity of the transmitted signal at wavelengths ranging from 2.1 to 3.5 μm. The dots represent the raw measurements and the solid lines show their smoothing. Blue colour represents the result of the signal passing through free space without a silica rod; green - with a 5 cm rod; red - with a 10 cm rod.

$$\tau(\omega) = \tau_0 \sqrt{1 + \frac{8a(\omega)Lln2}{\tau_0^2}}, \tag{2}$$

where $\tau_0 = 100$ fs is the duration of the pulse before entering the rod; L is the rod's length; $a(\omega) \equiv \frac{1}{2}\frac{d^2k}{d\omega^2}$ is a frequency-dependent parameter related to GVD of the silica rod, where a wave-vector, k, depends on a frequency, ω, according to a dispersion relation of silica. In the following we show that the parameter $a(\omega)$ can be reconstructed from the ToF measurement shown in Fig. 3.

The signal recorded by the MCT detector can be presented as a convolution of the system response function $g(\omega; t-t')$ with the signal pulse after the rod $f(\omega; t')$:[17]

$$(f(\omega) * g(\omega))(t) \equiv \int_0^\infty f(\omega; t')g(\omega; t-t'))dt'. \tag{3}$$

Because the response function, $g(\omega; t)$, is known (shown as the blue line in Figs. 3), the signal pulse emerging from the rod, $f(\omega; t)$ can be reconstructed using a deconvolution procedure.[18] For the deconvolution we used the smoothed results, shown as the solid lines, to avoid problems related to the noise present in the input functions. The reconstructed pulse is shown in Figs. 4 for different signal frequencies and rod lengths. It can be seen clearly by comparison of Fig. 4(a) and (b) that the pulse duration increases as the length of the rod was doubled. As well, the pulse broadens as the wavelength increases as expected for silica, a material with negative chromatic dispersion at this wavelength range.[19]

Furthermore, using Eq. 2 we calculated the GVD parameter, a, which is shown in Fig. 5(b) besides the corresponding pulse duration (Fig. 5(a)). To confirm the validity of our result it is informative to compare them to the literature. However, the published data has very limited information on GVD in the SWIR/MWIR range measured by the ultrafast pulses. Thus, we were restricted to judge our results against those made with a Continuous Wave (CW) source published elsewhere.[19–21] It can be seen that our ToF measurements using the ultrafast light laser reproduce well qualitatively the GVD which tends to increase as a function of the wavelength. However, the values obtained by us are greater by a factor of $\sim$2.5 in comparison to the CW results. At this stage, it is not clear whether the discrepancy arises from significantly different light sources or dissimilarity of silica materials used in the compared studies. We leave the discussion of this point out of the arguments in this report, as it deviates away from the work's main point.

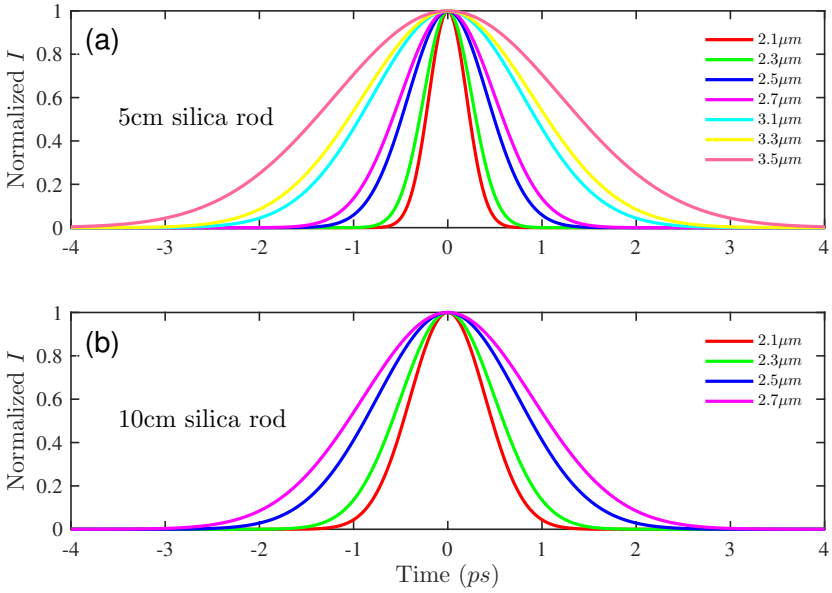

Figure 4. The signal pulse after silica rod as reconstructed by the deconvolution procedure. (a) and (b): for 5 and 10 cm long silica rods, respectively.

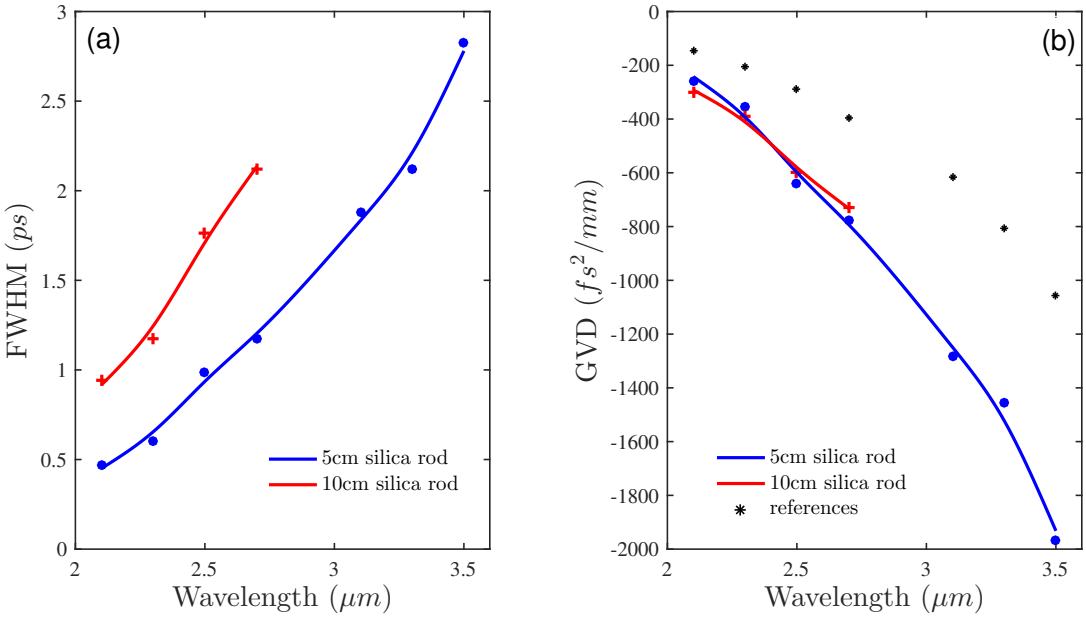

Figure 5. (a): the duration of the 100 fs pulse after stretching by the 5 and 10 cm long silica rods, blue and red dots, respectively. (b): The GVD of silica, red and blue dots are measured in this work using ToF method, black - taken from the references.[19–21] The lines are shown to guide the eye.

4. CONCLUSION

We have demonstrated that an all-optical modulator in combination with an MCT detector can be used for the high resolution ToF measurements. We have shown that the resolution is limited by the duration of the rising edge of the modulator response. Because the modulator response time is underpinned by electronic excitation driven by an external optical pulse source, its response time is as fast as that of the pump source and we have shown that the temporal resolution as fast as 100 femtosecond can be achieved. With the demonstrated speed of modulation it is possible to achieve the spatial resolution of $D = \frac{1}{2}ct = 1.5 \times 10^{-3}$ cm (c is the speed of light and t is the temporal resolution), suitable for the most demanding applications.

To demonstrate the feasibility of all-optical modulation for ToF measurements with a commercial MCT detector, we performed measurements in SWIR/MWIR range of 100 femtosecond pulse broadening traversing the silica rod. We show that it is not only possible to reconstruct the duration of the pulse broadened after the propagation through the rod, but it is possible to deduce the GVD of the material, a measurement which was not previously performed with ultrafast source in SWIR/MWIR regime.

ACKNOWLEDGMENTS

The authors acknowledge financial support provided by The Quantum Enhanced Imaging Hub (QuantIC) and EPSRC UK.

REFERENCES

1. R. Lange and P. Seitz, "Solid-state time-of-flight range camera," *IEEE Journal of Quantum Electronics* **37**, pp. 390–397, March 2001.
2. P. Besl, "Active optical range imaging sensors," *Machine Vision and Applications* **1**(2), pp. 127–152, 1988.
3. R. G. Dorsch, G. Hausler, and J. M. Herrmann, "Laser triangulation: Fundamental uncertainty in distance measurement," *Appl. Opt.* **33**, pp. 1306–1314, 1994.
4. K. Määttä, J. Kostamovaara, and R. Myllylä, "Profiling of hot surfaces by pulsed time- of-flight laser range finder techniques," *Appl. Opt.* **32**(27), pp. 5334 – 5347, 1993.
5. M. Koskinen, J. Kostamovaara, and R. Myllylä, "Comparison of the continuous wave and pulsed time-of-flight laser rangefinding techniques," *Optics, Illumination and Image Sensing for Machine Vision VI, Proc. SPIE* **1614**, pp. 296–305, 1992.
6. J. F. Andersen, J. Busck, and H. Heiselberg, "Applications of high resolution laser radar for 3-d multispectral imaging," *Proc.SPIE* **6214**, p. 28, 2006.
7. J. D. Beck, C. F. Wan, M. A. Kinch, and J. E. Robinson, "MWIR HgCdTe avalanche photodiodes," *Proc. SPIE* **4454**, pp. 188–197, 2001.
8. J. B. Abshire, A. Ramanathan, H. Riris, J. Mao, G. R. Allan, W. E. Hasselbrack, C. J. Weaver, and E. V. Browell, "Airborne measurements of co_2 column concentration and range using a pulsed direct-detection ipda lidar," *Remote Sens.* **6**(1), pp. 443–469, 2013.
9. A. Kaplan and D. Chekulaev, "Optical absorber," Mar. 14 2017. US Patent 9,594,265.
10. S. J. Park, A. Zakar, V. L. Zerova, D. Chekulaev, L. T. Canham, and A. Kaplan, "All-optical modulation in mid-wavelength infrared using porous si membranes," *Scientific Reports* **6**, p. 30211, 2016.
11. A. Zakar, S. J. Park, V. Zerova, A. Kaplan, L. T. Canham, K. L. Lewis, and C. D. Burgess, "MWIR optical modulation using structured silicon membranes," *Proc. SPIE* **9992**, p. 7, 2016.
12. J. B. Heaney, K. P. Stewart, and G. Hass, "Transmittance and reflectance of crystalline quartz and high- and low-water content fused silica from 2 μm to 1 mm," *Appl. Opt.* **22**(24), pp. 4069–4072, 1983.
13. A. Zakar, R. Wu, D. Chekulaev, V. Zerova, W. He, L. Canham, and A. Kaplan, "Carrier dynamics and surface vibration-assisted auger recombination in porous silicon," *Phys. Rev. B* **97**, p. 155203, Apr 2018.
14. W. He, I. V. Yurkevich, L. T. Canham, A. Loni, and A. Kaplan, "Determination of excitation profile and dielectric function spatial nonuniformity in porous silicon by using wkb approach," *Opt. Express* **22**(22), pp. 27123–27135, 2014.
15. C. Levy-Clement, A. Lagoubi, and R. Tenne, "Photoelectrochemical etching of silicon," *Electrochimica Acta* **37**(5), pp. 877–888, 1992.

16. A. Yariv and P. Yeh, *Photonics*, Oxford University Press, 6th ed., 2007.
17. J. D. Irwin, *The Industrial Electronics Handbook*, CRC Press, 1st ed., 1997.
18. T. C. O'Haver, *A Pragmatic Introduction to Signal Processing: with applications in scientific measurement*, CreateSpace Independent Publishing Platform, 2nd ed., 2016.
19. I. H. Malitson, "Interspecimen comparison of the refractive index of fused silica," *J. Opt. Soc. Am.* **55**, pp. 1205–1209, Oct 1965.
20. C. Tan, "Determination of refractive index of silica glass for infrared wavelengths by ir spectroscopy," *Journal of Non-Crystalline Solids* **223**(1), pp. 158 – 163, 1998.
21. T. Radhakrishnan, "Further studies on the temperature variation of the refractive index of crystals," *Proc. Indian Acad. Sci.* **31**, pp. 22–34, 1951.